Journal of ELECTRICAL ENGINEERING, VOL 59. NO 7/s, 2008, 97-102

MAGNETIC MODELLING OF GMR HYSTERESIS AND APPLICATIONS OF THE MODELLING

Martin Sablik* — Luc Dupre**

In the past several years, there has been some interest in modelling hysteresis in giant magnetoresistance (GMR) as a function of magnetic field in magnetic multilayer films. The purpose of this paper is to review work published a decade ago on such modelling and on application of such modelling to the design of a GMR field sensor. The computed GMR curves qualitatively reproduce the GMR hysteresis seen experimentally. In particular, two GMR peaks are found to be symmetrically placed about $H = 0$, and the GMR hysteresis curve itself is found to have an inverted butterfly shape. In the model, the hysteresis derives from the hysteretic dependence of the magnetization and from an essentially quadratic dependence of the change in the magnetoresistance on the magnetization. Multilayered films were treated as having a resistivity of different layers in parallel. Discontinuous multilayer films were treated as having blocks of magnetic and nonmagnetic material in series within the discontinuous layers. In the original model, a variant of the Jiles-Atherton model was used for the hysteresis in the magnetization. In fact, other hysteresis models for the magnetization could be used, on which the magnetoresistance then depends. A particular application utilized the Schneider model for the magnetic hysteresis and computed GMR from that for the purpose of using the modelling as a guide for designing a GMR magnetic field sensor with a minimum of magnetic noise in its measurements. In that modelling, the magnetic Barkhausen noise was computed at each point in the hysteresis cycle of the magnetic field. It was found that the magnetic noise was largest near the coercive field, but in fact the GMR decreased linearly from its peaks on both sides of $H = 0$ to fields well away from H_c, which indicated that the GMR could follow the field linearly in a region with very minimal magnetic noise. Thus, to produce the field sensor, a bias field is to be applied.

Keywords: giant magnetoresistance hysteresis, modelling, application to magnetic noise in GMR field sensors

1 INTRODUCTION

The phenomenon of giant magnetoresistance (GMR) was first discovered in Fe/Cr multilayered film structures with antiferromagnetic coupling between the Fe layers, [1-3]. In the GMR effect, the resistivity of the film structure changes markedly (as much as by 30-50% at 4 K) when a magnetic field is applied.

GMR [4-6] is related to the realigning of the spin magnetic moments of the electrons in the magnetic part of the film in an applied magnetic field. If the field is large enough, the Fe layers become ferromagnetically aligned. Conduction electrons with spins parallel to the aligned Fe spins go through the entire structure much more readily than conduction electrons with antiparallel spins, which tend to scatter much more strongly both in the iron and in the interface between iron and chromium.

The magnetic component of the film could even be an alloy, such as in NiFe/Cu, [7,8] where NiFe is permalloy. This film is significant because it exhibits 2-4% GMR at room temperature. Another discovery was that the magnetic layers could be uncoupled instead of ferromagnetically coupled and still have GMR.

Finally, GMR was found in granular films, *ie* in films with magnetic particles embedded in a nonmagnetic host matrix such as in Co-Cu, Fe-Cu, Co-Ag, and Fe-Ag, [9-12]. Such films are easier and cheaper to make, but the fields necessary to produce the desired effect were a bit too large (8-25kA/m) for use in devices.

New developments were “discontinuous multilayers”, [13-16]. Such films exhibit fairly large room temperature GMR (~5%) in lower applied fields (4-8 kA/m). Such a film was produced by first sputtering NiFe/Ag and then annealing at 335 C. The annealing broke magnetic layers into magnetic islands with inter-layer material between them. The film behaves like a granular film, but where “magnetic particles” are large enough not to increase the coercivity of the film. This means that the half-width of the GMR peak (or rather of the GMR double peak because of hysteresis about $H = 0$) is very narrow.

The model discussed in this paper was used to predict GMR and its hysteresis in discontinuous multilayer films, [17]. It was the first model to treat hysteresis in GMR. The model with some modifications was then used to map the effects of GMR hysteresis on the accompanying magnetic noise in a GMR field sensor, and design the field sensor so as to minimize the magnetic noise, [18].

We review this modelling work at this time because recently GMR hysteresis has been modelled with the Preisach model [19-21] instead of the Jiles-Atherton-Sablik model [22] or the Schneider model [23], as in the original work [17, 18]. There is such a time space between works that it is important to review.

2 GMR MODEL FORMULATION

The model assumes the following:

(1) Both current density and applied magnetic field are parallel to the film layers. This is the “current in plane” (CIP) configuration.
(2) Circuit-wise, the layers are connected in parallel. This neglects current flow back and forth between layers.

* Southwest Research Institute, PO Drawer 28510, San Antonio, TX 78228-0510 and AM-PM, LLC, San Antonio, TX 78240-2307; msablik@swri.org
** Department of Electrical Engineering, University of Ghent, Ghent, Belgium; luc.dupre@ugent.be

ISSN 1335-3632

(3) At the top and bottom of the film structure are nonmagnetic over- and underlayers of greater thickness T than the multilayers.
(4) For discontinuous multilayers, the magnetic layers are broken into islands and in between the islands there is nonmagnetic material from the nonmagnetic layers.
(5) The boundary between magnetic islands and nonmagnetic material is broadened into a mixed region of interface material. Camblong [24,25], for example, uses this approach as a model for interfaces between layers. Clearly, the interface material will be some kind of alloy material between the magnetic and the nonmagnetic material.

A diagram of the model for the film structure is seen in Fig. 1a, and a diagram of the spacing between islands is seen in Fig. 1b. In the model, the spacing between islands resembles a "channel" of nonmagnetic material with two mixed interface regions forming "beaches" for the magnetic islands on either side of the "channel."

Since the various layers act as resistances in parallel, we have for the total resistance R

$$\frac{1}{R} = \frac{n-1}{R_N} + \frac{2}{R_c} + \frac{\mathrm{n}}{R_m^d} \qquad (1)$$

where R_N is the resistance of each nonmagnetic layer, R_m^d is the resistance of each discontinuous magnetic layer, and R_c is the resistance of the top or bottom capping layer, with top and bottom assumed to be of the same length and width and of the same material as the nonmagnetic layers. There are n magnetic layers and n-1 nonmagnetic layers.

In each magnetic layer, the magnetic islands, nonmagnetic channels, and mixed interface regions are electrically connected in series, so that

$$R_m^d = R_M \frac{(m+1)L}{D} + R_{NC} \frac{mL_C}{D} + R_I \frac{2mL_I}{D} \qquad (2)$$

where there are 2m interfaces and m channels, where the film has length D in the direction of current and field, where R_M is the resistance of the magnetic island material, R_NC is the resistance of the normal material in the channel and where R_I is the resistance of the mixed interface region. Each magnetic island has length L; each interface, length L_I; each channel of normal material, length L_C.

The resistances R_M, R_NC, R_I and R_N are given as

$$R_M = \rho_M \frac{D}{wt_M}, \qquad R_{NC} = \rho_N \frac{D}{wt_M},$$
$$R_I = \rho_I \frac{D}{wt_M}, \qquad R_N = \rho_N \frac{D}{wt}, \qquad (3a,b,c,d)$$

where the film has width w, the magnetic layers have thickness t_M and normal layers, thickness t.

The resistivities of the magnetic material, the normal material and interface material are ρ_M, ρ_N, and ρ_I respectively. One can then define the net resistivity ρ_net of the entire discontinuous layer structure by the relationship.

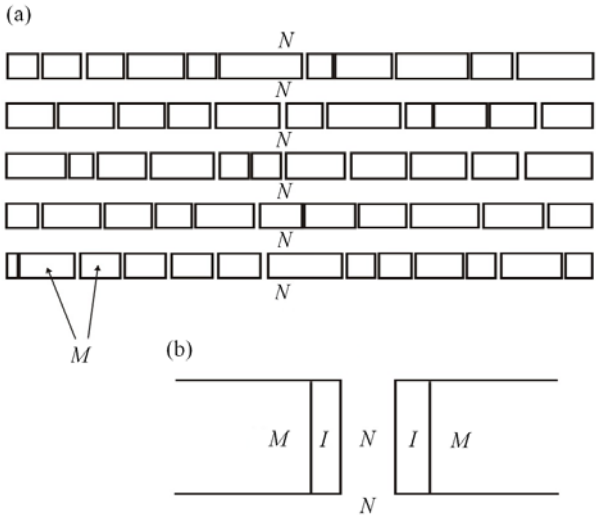

Fig. 1. (a) - Schematic diagram of a discontinuous multiplayer film structure. *N* stands for nonmagnetic or "normal" metal. *M* stands for magnetic metal. Field *H* and current density *j* are parallel to the layer structure.
(b) - Close-up of space between two magnetic islands in one of the magnetic layers. Normal material fills up part of the space between islands and interface layer material *I* fills up the rest, forming "beaches" of *I* material on the edge of each magnetic island.

$$\frac{1}{R} = w\frac{(n-1)t + 2T + nt_M}{\rho_{net} D} \qquad (4)$$

The GMR ratio is then defined as

$$\mathrm{GMR} = \frac{\rho_{net}(M) - \rho_{net}(M_s)}{\rho_{net}(0)} \qquad (5)$$

where $\rho_\mathrm{net}(0)$ is the net resistivity at zero field, $\rho_\mathrm{net}(M)$ is the net resistivity at field H and magnetization M, and $\rho_\mathrm{net}(M_\mathrm{s})$ is the net resistivity at saturation magnetization.

A perusal of the literature suggested the following for the relationship with magnetization for the resistivity:

$$\rho_M(M) = \rho_M(0) + \left[\rho_M(M_s) - \rho_M(0)\right]\left|\frac{M}{M_s}\right|^{\upsilon} \qquad (6)$$

where |.| denotes the absolute value and where the power υ depends on the situation.

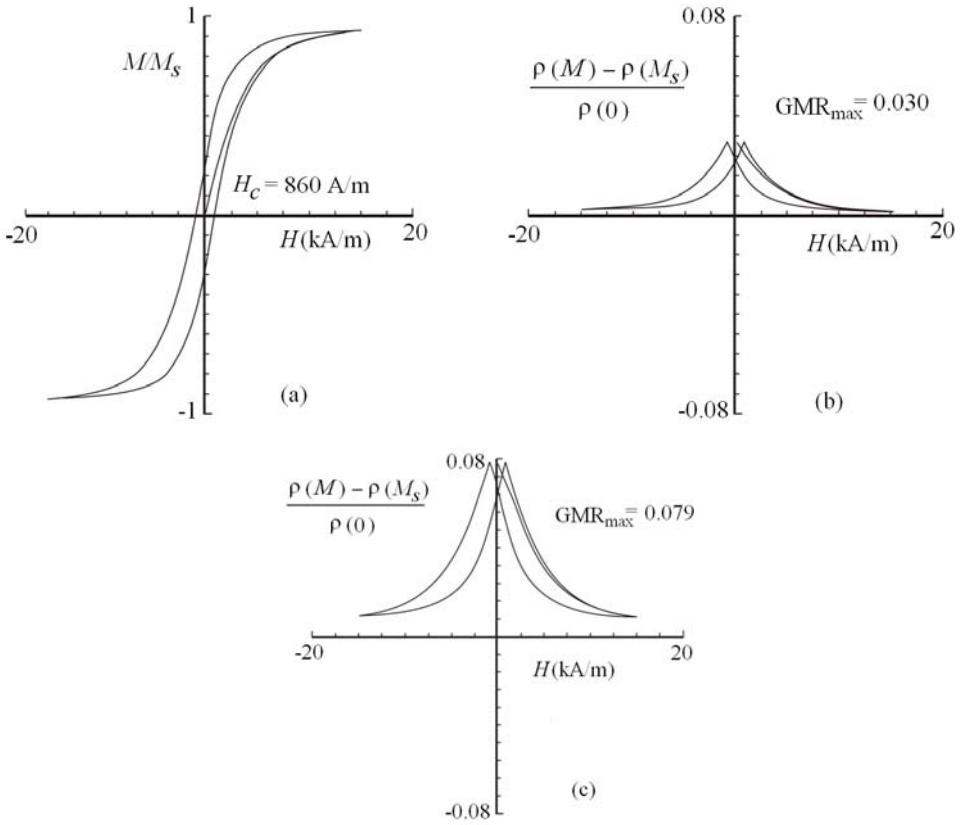

Fig. 2. (a) − Hysteresis curve, as computed by the Sablik-Jiles model, [22]. Hysteresis parameters were M_s = 1.685 MA/m, a = 875 A/m, k/μ_0 = 1950 A/m, c = 0.435, and λ_s = 8.14×10^{-6}; (b) − GMR hysteresis curve computed for an un-annealed multilayer film with magnetic hysteresis as in (a); (c) − GMR hysteresis curve for an annealed discontinuous multilayer film with same GMR parameters as in (b) and with magnetic hysteresis as in (a).

For the ferromagnetic metal layer, Smit [26] and later McEwen [27] describe the resistance of ferromagnetic metals as being linearly dependent on flux density B, which means that since $M >> H$, $\rho(M)$ is linearly dependent on M and υ=1. This was used in the original paper for the magnetic layer. For the interface alloy material, υ = 2, υ = 1 and υ = 1/2 were used.

The ν = 2 is consistent with the behaviour of many magnetic alloys, [28]-[33]. For amorphous alloys, υ can vary between a fraction less than one and a value less than or equal to 2, [34]-[38].

The magnetization M is computed from a hysteresis model for magnetization. For the discontinuous multilayer films, the Jiles-Atherton-Sablik model [22] was used. Later, when we treated the magnetic field sensor problem, a regular multilayer film was modelled, and for the hysteresis, the Schneider model [23] was used. Also, υ = 2 was used for the magnetic layer. In every case, for the nonmagnetic layer, ρ_N is constant and not dependent on magnetization of the magnetic layer.

The model produces two GMR peaks, positioned at a field equal to the coercivity. The width of the GMR hysteresis depends on the hysteresis parameters. The GMR ratio amplitude depends on the GMR parameters. Figure 2 shows, for a specific modelled hysteresis curve, as seen in part (a), that a modelled GMR curve for continuous layers, as seen in part (b), will develop a larger amplitude GMR curve when the modelled layer is made discontinuous, as seen in part (c).

COMPUTATION OF MAGNETIC NOISE

By magnetic noise, we mean here magnetic Barkhausen noise. A model for that was derived originally by Alessandro *et al* [39] and then extended to a magnetic field dependence, [40,41].

The model was originally derived by considering the motion of a 180-degree domain wall and by employing a set of coupled Langevin equations, which are differential equations incorporating a stochastic (or randomly varying) forcing term. The equations were solved for a noise spectral distribution function as a function of frequency. Sablik [40,41] then integrated this result to obtain the magnetic noise amplitude as a function of magnetic field. This noise amplitude (in watts) gives a

measure of magnetic fluctuations due to flux changes resulting from sudden motions of domain walls, which slip from one pinning site to the next as field increases.

The integrated result for the magnetic Barkhausen noise amplitude J in watts at field H is

$$J = \frac{2S^3\dot{M}A\mu^2\tau'_c}{\pi\mu_0(\tau'^2-\tau'^2_c)\tau'}\times \\ \times\left\{\tau'\left[\arctan(\omega_{\max}\tau'_c)-\arctan(\omega_{\min}\tau'_c)\right]\right. \\ \left.-\tau'_c\left[\arctan(\omega_{\max}\tau')-\arctan(\omega_{\min}\tau')\right]\right\} \quad (7)$$

which is the equivalent of (14) in [41]. The primed time constants differ from those in [41] in that

$$\tau' = \frac{\mu_0\tau}{\mu D_m}, \quad \tau'_c = \frac{\mu D_m\tau_c}{\mu_0^2} \quad (8a,b)$$

where D_m is a constant associated with demagnetization field $-D_mM$. Equation (7) is derived in the same way as (14) in [41] but this time (7) in [39] is

$$\frac{d\Phi}{dt}+\frac{\mu D_m\Phi-\mu_0^2S\dot{M}}{\tau\mu_0} = -\frac{\hat{H}_c}{\sigma G} \quad (9)$$

which equates the "magnetostatic field" in [41] with demagnetization field, and which assume

$$B=\mu_0(H_{app}+M), \quad \mu=\frac{dB}{dH_{app}}, \\ H=H_{app}-D_mM, \quad \Phi=BS. \quad (10a,b,c,d)$$

The time constants τ and τ_c are as in [41], namely,

$$\tau=\sigma GS\mu, \quad \tau_c=\frac{\xi}{S\dot{M}} \quad (11a,b)$$

and the rest of the symbols are defined as in [39]. Equation (9) results in a noise power spectrum which, integrated across frequency, leads to the result in (7).

To obtain the noise amplitude $J(H)$ as a function of H, one substitutes the H-dependent result for $\mu(H)$ from a magnetic hysteresis model. For this particular work, the Schneider model [23] was used to obtain $\mu(H)$ instead of the Sablik-Jiles model, [22]. In the case of the Schneider model, the curve generated at zero stress (if input hysteresis data are inputted correctly), is always a regurgitation of the experimental hysteresis curve, except for a little smoothing. Since the magnetic hysteresis of the GMR material had a somewhat unusual shape (see Fig. 3), it was thought best to use the Schneider model since it would generate almost the same shape. Note that since the Schneider model does not compute an expression for the irreversible permeability $\mu_{irr}(H)$, the total permeability $\mu(H)$ was substituted into (7) instead of $\mu_{irr}(H)$ as in [41] and as in the earlier [40].

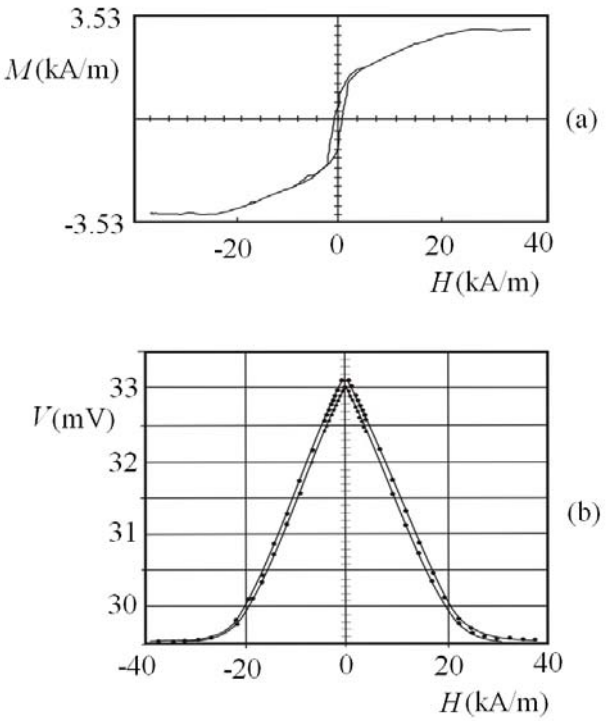

Fig. 3. (a) - Experimental magnetic hysteresis curve for the GMR mutilayer material; (b) - Experimental GMR hysteresis curve for the same multiplayer material

4 APPLICATION TO GMR FIELD SENSORS

The model for the GMR field sensor assumes that the multilayer material of the sensor has magnetic layers alternating with nonmagnetic layers with an overlayer and underlayer of nonmagnetic material, just as in section 2. But, in this case, the magnetic layers are continuous, not discontinuous. Circuit-wise, the layers are all in parallel, and the magnetic layers are assumed to have a resistivity dependent on the magnetization as

$$\rho_m(M) = \rho_m(0)+\left[\rho_m(M_s)-\rho_m(0)\right]\left(\frac{M}{M_s}\right)^2 \quad (12)$$

The expression for the net resistivity ρ_{net} of the film and the GMR ratio are found as in section 2. Since the GMR ratio is then a function of $M(H)$, and since $M(H)$ exhibits hysteresis, so also does the GMR.

Figures 4a to 4d show computed magnetic hysteresis (B *vs* H), relative permeability hysteresis (μ_r *vs* H), Barkhausen noise hysteresis (J *vs* H), and GMR hysteresis (GMR *vs* H). For these data, the demagnetization constant D_m was set to 1 (because the field was in the plane of the film). Also, electrical conductivity $\sigma=5\times 10^6$ $(\Omega m)^{-1}$, and $S=5\times10^{-9}$ m^2 was used for average domain wall area. The rest of the constants substituted into the Barkhausen calculation are as in [41]. For the GMR calculation, whatever constants from [17] that apply were used in this calculation.

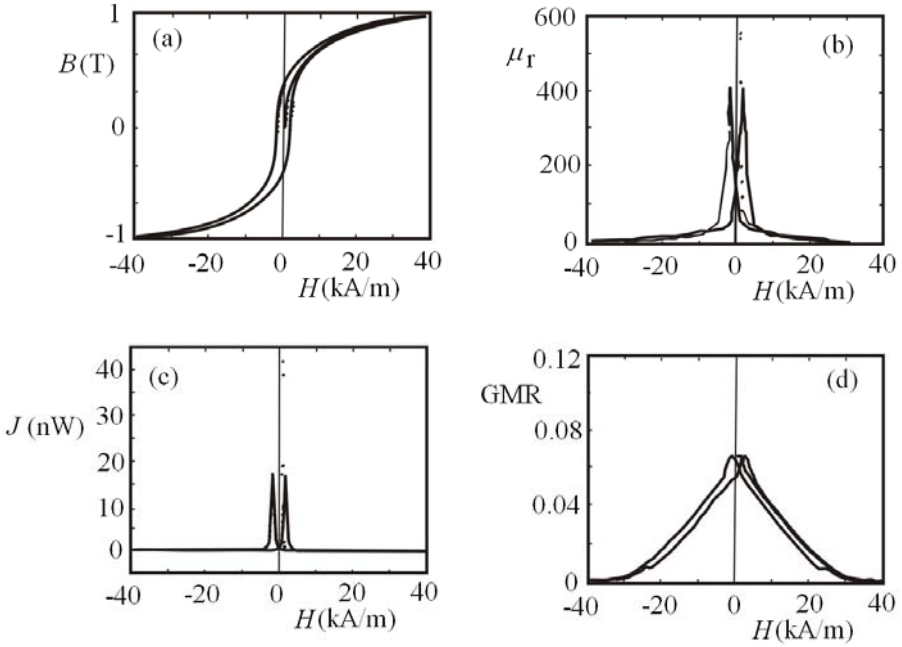

Fig. 4. Four computed characteristics for the GMR multilayer material are shown: (a) - *B vs H*; (b) - μ *vs H*; (c) - *J vs H*; and (d) - GMR *vs H*

It was noted that a much smaller maximum permeability (by two orders of magnitude) for the GMR material than permalloy results in maximum Barkhausen noise amplitude *J* that is dramatically decreased by six orders of magnitude. Thus, it was recommended that permalloy concentrators are too noisy to be used in a GMR field sensing device and that another design is preferable (which has since then led to a new design which is now successfully tested).

Figure 4d shows the simulated GMR behaviour. This shows the linear region and the two parallel increasing and decreasing portions of the GMR curve. The latter are a little more exaggerated than in Fig. 3b owing to the smoothing of the experimental magnetic hysteresis curve that had to be accomplished.

Also, because of the values selected for the parameters, the maximum GMR is computed to be 7%, whereas the experimental maximum GMR is 11%. A better quantitative fit is possible with better parameter selection. The important point here is the qualitative similarity of Fig. 4d and Fig. 3b and the appearance of the linear range in GMR *vs H*.

Furthermore, it is noted from Fig. 4c that the magnetic noise is maximum in the vicinity of H_c (10 kA/m for the multilayer material), but that the device can be operated well away from where the noise is located by applying a bias field, so that the GMR response to an external field is linear and not affected by the noise near H_c.

5 CONCLUSIONS

In this presentation, it is reminded that GMR hysteresis was first modelled in the late 1990s. The first manifestation of this modelling was to model GMR hysteresis for discontinuous multilayer films. Not only the shape of the GMR curve with two symmetric peaks near $\pm H_c$ is reproduced, but also increase in GMR amplitude is found in GMR discontinuous multilayer films with the magnetic layers broken into "magnetic" islands. A later application was to model the magnetic noise and the GMR of a GMR magnetic field sensor. For the particular sensor in question, the model produced a GMR hysteresis curve with a linear region that extended well away from H_c, which was the region of very large magnetic noise, according to the modelling. Thus, it became clear that a bias field was needed in order to operate the device so that a field change resulted in a linear change in the sensed voltage without any appreciable noise. It was also shown that the permalloy field concentrators had to be replaced by a material with a lower permeability in order to reduce the magnitude of the overall magnetic noise.

REFERENCES

[1] BABICH, M.N. – BROTO, J. M. – FERT, A. – DAU, N.V. – PETROFF, F. – ETIENNE, P. – CREUZET, G. – FRIEDERICH, A. – CHAZELAS, J..: Giant Magnetoresistance of (001)Fe/(001)Cr Magnetic Superlattices, Phys. Rev. Lett. **61** (1988), 2472-2475

[2] BINASCH,G. – GRUNBERG,P. – SAURENBACH,F. – ZINN,W.: Enhanced Magnetoresistance in Layered Magnetic Structures wit Antiferromagnetic Interlayer Exchange, Phys. Rev. B **39** (1989), 4828-4830

[3] KREBS,J. – LUBITZ,P. – CHAIKEN,A.– PRINZ,G.A.: Magnetic Resonance Determination of the Antiferromagnetic Coupling of Fe Layers through Cr, Phys. Rev. Lett. **63** (1989), 1645-1648

[4] LEVY,P.M. – ZHANG,S. – FERT,A.: Electrical Conductivity of Magnetic Multilayered Structures, Phys. Rev. Lett. **65** (1990), 1643-1646

[5] BARNAS,J. – FUSS,A. – CAMLEY,R.E. – GRUNBERG,P. – ZINN,W.: Novel Magneoresistance Effect in Layered Magnetic Structures: Theory and Experiment, Phys. Rev. B **42** (1990), 8110-8120

[6] BARTHELEMY,A. – FERT,A.: Theory of the Magnetoresistance in Magnetic Multilayers: Analytical Expressions from a Semiclassical Approach, Phys. Rev. B **43** (1991), 13124-13129

[7] DIENY,B. – SPERISOU,V.S. – METIN,S – PARKIN,S.S.P. – GURNEY,B.A. – BAUMGART,P. – WILHOIT,D.R.: Magnetotransport Properties of Magnetically Soft Spin-Valve Structures, J. Appl. Phys. **69** (1991), 4774-4779

[8] DIENY,B. – SPERISOU,V.S. – PARKIN,S.S.P. – GURNEY,B.A. – WILHOIT,D.R. – MAURI,D.: Giant Magnetoresistance in Soft Ferromagnetic Multilayers, Phys. Rev. B **43** (1991), 1297-1300

[9] BERKOWITZ,A.E. - MITCHELL,J.R. – CAREY,M.J. – YOUNG,A.P. – ZHANG,S. – SPADA,F.E. – PARKER,F.T. – HUTTEN,A. – THOMAS,G.: Giant Magnetoresistance in Heterogeneous Cu-Co Alloys, Phys. Rev. Lett**. 68** (1992), 3745-3748

[10] ZIAO.J.Q. – JIANG,J.S. – CHIEN,C.L.: Giant Magnetoresistance in Non-Multilayer Magnetic Systems, Phys. Rev. Lett. **68** (1992), 3749-3752

[11] CAREY,M.J. – YOUNG,J.P. – STARR,A. – RAO,D. – BERKOWITZ,A.: Giant Magnetoresistance in Heterogeneous AgCo Alloy Films, Appl. Phys. Lett. **61** (1992), 2935-2937

[12] TSOUKATOS,A. – WAN,H. – HADJIPANAYIS,G.C. – LI,Z.G.: Giant Magnetoresistance in Magnetically Inhomogeneous Thin Films, Appl. Phys. Lett. **61** (1992). 3059-3061

[13] HYLTON,T.L. – COFFEY,K.R. – PARKER,M.A. – HOWARD,J.K.: Giant magnetoresistance at Low Fields in Discontinuous NiFe-Ag Multilayer Thin Films, Science **261** (1993), 1021-1024

[14] HYLTON,T.L. – COFFEY,K.R. – PARKER,M.A. – HOWARD, J.K.: Low Field Giant Magnetoresistance in Discontinuous Magnetic Multilayers, J. Appl. Phys. **75** (1994) 7058-7060

[15] PARKER,M.A. – HYLTON,T.L. – COFFEY.K.R. – HOWARD,J.K.: Microstructural Origin of Giant Magnetoresistance in a New Sensor Structure Based on NiFe/Ag Discontinuous Multilayer Films, J. Appl. Phys. **75** (1994), 6382-6384

[16] SNOECK,E. – SINCLAIR,R. – PARKER,M.A. – HYLTON.T.L. – COFFEY,K.R. – HOWARD,J.K. – LESSMAN,A. – BIENENSTOCK,A.I.: Microstructural Evolution of NiFe/Ag Multilayers Studied by X-Ray Diffraction and In-Situ High-Resolution TEM, J. Magn. Magn. Mater. **100** (1995), 24-32

[17] SABLIK,M.J.: A Phenomenological Model for Giant Magnetoresistance Hysteresis in Magnetic Discontinuous Multilayer Films, IEEE Trans. Magn. **33** (1997), 2375-2385

[18] SABLIK,M.J. – BEECH,R.S. – TONDRA,M.: Designing a Giant Magnetoresistance Field Sensor via Inferences from a Giant Magnetoresistance Hysteresis Model, J. Appl. Phys. **87** (2000) 5347-5349

[19] AC,V: Experimental Verification of Preisach Hysteresis Model in Layered GMR Structures, ASDAM 2004, 5th Intl. Conf. On Advanced Semiconductor Devices and Microsystems, Smolenice Castle, Slovakia, 2004.

[20] AC,V.: Application of the Preisach Model to Computation Behavioral Characteristics in GMR Structure, 12th Biennial IEEE Conference on Electromagnetic Field Computation Digest Book, Miami, FL, 2006, p.97 (CD-Rom)

[21] AC,V.: A Study of Hysteresis in the GMR Layer Structures by FEM, Physica B **403** (2008), 460-3

[22] SABLIK,M.J. – JILES,D.C.: Coupled Magnetoelastic Theory of Magnetic and Magnetostrictive Hysteresis, IEEE Trans. Magn. **29** (1993), 2113-2123

[23] SCHNEIDER,C.S. – CANNELL,P.K. – WATTS,K.T.: Magnetoelasticity for Large Stresses, IEEE Trans. Magn. **28** (1992), 2626-2631

[24] CAMBLONG,H.E.: Linear Transport Theory of Magnetoconductance in Metallic Multilayers: A Real-Space Approach, Phys. Rev. B **51** (1995), 1855-1865

[25] CAMBLONG,H.E. – LEVY,P.M. – ZHANG,S.: Electron Transport in Magnetic Inhomogeneous Media, Phys Rev. B **51** (1995), 16052-16072

[26] SMIT.J.: Magnetoresistance of Ferromagnetic Metals and Alloys at Low Temperatures, Physica **17** (1951), 612-627

[27] McEWEN,K.A. – WEBBER,C.D. – ROELAND,J.W.: Magnetoresistance of Gadolinium, Physica **86-88B** (1977), 531-532

[28] YOSIDA,K.: Anomalous Electrical Resistivity and Magnetoresistance due to an s-d Interaction in Cu-Mn Alloys, Phys. Rev. **107** (1957), 396-403

[29] MYDOSH,J.A. – ROTH,S.: High-Field Magnetization of PdMn and PdFeMn Spin-Glass Ferromagnetic Alloys, Phys. Lett. **69A** (1979), 350-352

[30] GENICON,J.L. – LAPIERRE,F. – SOULERIE,J.: Magnetoresistance of Dilute Alloys at Absolute Zero: The PdNi Case, Phys. Rev. B **10** (1974), 3976-3982

[31] SENOUSSI, S. – HAMRIC,A. – CAMPBELL,J.A.: The Influence of Magnetic Ordering on the Resistivity of PdMn Alloys, J. Phys. F **10** (1974) 3976-3982

[32] MERTIG,L. – MROSAN,E.: Magnetoresistivity of Metals: II. Application to 3d Transition Metal Impurities in Cu," J. Phys. F **13** (1983), 373-381.

[33] VINOKURA,L.I. – IVANOV,V.Yu.: Kinetic Properties of Iron-Rhodium Alloys in the Transition Region from Antiferromagnetism to Ferromagnetism, in Magnetic Electric Structure of Transition Metal Alloys, eds: Veselago,V.G. and Vinokura, L.I. (Commack, NY, Nova Science Pueblo, 1988), 83-123

[34] ASAMOZA,R. – CAMPBELL,I.A. – FERT,A. – LIENARD,A. – REBOUILLAT,J.P.: Magnetic and Transport Properties of Nickel-Rare Earth Amorphous Alloys, J. Phys. F **9** (1979), 349-371

[35] LENZ,M.: Negative Magnetoresistivity in Antiferromagnetic BCC Cr-Al Solid Solutions, Phys. Stst. Sol. (a) **62** (1980), 223-228

[36] LEE,P.A. – RAMAKRISHMAN,T.V.: Magnetoresistance of Weakly Disordered Electrons, Phys.Rev. B **26** (1982), 4009-4012

[37] HOWSON,M.A. – GRIEG,D.: Magnetoresistance of Amorphous Metallic Alloys: Evidence for Coulombic Interaction Effects, J. Phys. F **13** (1983), L155-L158

[38] BIERI,J. – FERT, A. – CREUZET,G. – OUSSET,J.C.: Magnetoresistance of Amorphous Alloys: Weak Localization in Three-Dimensional Metallic Systems, J. Appl. Phys. **55** (1984), 1948-1950

[39] ALESSANDRO,P – BEATRICE,C. – BERTOTTI,G. – MONTORSI,A.: Domain-Wall Dynamics and Barkhausen Effect in Metallic Ferromagnetic Materials, J. Appl. Phys. **68** (1990) 2901-2905

[40] SABLIK,M.J.: A Model of Barkhausen Noise Power as a Function of Applied Magnetic Field and Stress, J. Appl. Phys. **74** (1993) 5898-5900

[41] SABLIK,M.J. – AUGUSTYNIAK,B.: The Effect of Mechanical Stress on a Barkhausen Noise Signal Integrated Across a Cycle of Ramped Mangetic Field, J. Appl. Phys. **79** (1996), 963-972

Received 19 September 2008